



## Research article

# Dexmedetomidine attenuates isoflurane-induced neuroapoptosis through the miR-137/GSK-3 $\beta$ pathway in the developing rat hippocampus<sup>☆</sup>

Xueyuan Hu<sup>a,1</sup>, Zihan Sun<sup>a,1</sup>, Wenjing Wang<sup>a</sup>, Gong Xiao<sup>b</sup>, Quanlin Yu<sup>a</sup>,  
Liang Chi<sup>a</sup>, Huanqi Liu<sup>a,\*</sup>

<sup>a</sup> College of Veterinary Medicine, Qingdao Agricultural University, Qingdao, 266109, China

<sup>b</sup> Animal Husbandry Development Promotion Center of Pingyi County, Linyi, 273300, China

## ARTICLE INFO

## Keywords:

Isoflurane  
Developing rats  
Hippocampal apoptosis  
Dexmedetomidine  
miR-137

## ABSTRACT

Long-term isoflurane inhalation has been reported to induce hippocampal apoptosis in young animals, whereas dexmedetomidine (DEX) can reduce isoflurane-induced neuronal apoptosis. The neuroprotective effect of miR-137 has been reported before, however, the effect of on isoflurane triggered neuronal apoptosis, and whether miR-137 is involved in the neuroprotection of DEX remain unclear. To investigate these doubts, we established an isoflurane exposure model in postnatal day 7 (P7) Sprague–Dawley rats and the PC12 cells, containing a control group (CON), isoflurane group (ISO), DEX group (DEX) and DEX pretreatment group (DEX + ISO). We first confirmed that DEX attenuates isoflurane-induced hippocampal apoptosis. And we found DEX increased miR-137 and attenuated GSK-3 $\beta$  levels in the DEX and DEX + ISO groups in the hippocampus and PC12 cells. In addition, the regulative relationship of miR-137 and GSK-3 $\beta$  was confirmed using the TargetScan tool and dual-luciferase reporter assay. Moreover, miR-137 overexpression inhibited GSK-3 $\beta$  and increased its downstream gene  $\beta$ -catenin, whereas knockdown of miR-137 changed the GSK-3 $\beta$  and  $\beta$ -catenin expression oppositely. Upregulation of miR-137 increased the apoptosis-related genes and decreased the anti-apoptosis gene; however, knockdown of miR-137 produced the opposite results. This study suggested that DEX attenuated isoflurane-induced neuroapoptosis by upregulating the miR-137 mediated GSK-3 $\beta$ / $\beta$ -catenin pathway in the developing rat hippocampus.

## 1. Introduction

Isoflurane is one of the most commonly used inhalation anesthetics for various surgeries in animals and humans. However, studies have shown that isoflurane has certain neurotoxicity, especially for developing animals, because neurons in the developing period are very vulnerable [1,2]. Isoflurane inhalation may cause long-term developmental neurotoxicity and induce extensive neuronal apoptosis in the neonatal brain, leading to subsequent continuous learning and memory disorders [3,4]. Although the literature has

<sup>☆</sup> All the authors have read and agreed to submit the manuscript in this version.

\* Corresponding author. No. 700 Great Wall Road, Chengyang District, Qingdao, 266109, China.

E-mail address: [huanqiliu@126.com](mailto:huanqiliu@126.com) (H. Liu).

<sup>1</sup> These authors contributed equally to this work.

<https://doi.org/10.1016/j.heliyon.2024.e31372>

Received 17 January 2024; Received in revised form 11 May 2024; Accepted 15 May 2024

Available online 16 May 2024

2405-8440/© 2024 Published by Elsevier Ltd. This is an open access article under the CC BY-NC-ND license (<http://creativecommons.org/licenses/by-nc-nd/4.0/>).

shown that the risk of anesthetic neurotoxicity could be ignored in early routine surgery in human medical clinics [5], animal experiments have shown that long-term exposure to isoflurane induced neurotoxicity and increased nerve cell death in young animals. The hippocampus is one of the targets of isoflurane. Long-term exposure to isoflurane could promote hippocampal neuron apoptosis, damage the learning and memory ability of rats, reduce the survival rate, and result in cognitive dysfunction [6,7], whereas how isoflurane triggers neuron apoptosis remains unclear. microRNAs (miRNAs) are a class of small noncoding RNAs about 20 nucleotides (nt) in length that participate in cell proliferation, differentiation and apoptosis and other cell processes gene in the central nervous system [8]. For example, microRNA (miR)-124 contributes to neurogenesis by downregulating the REST/SCP1 pathway during embryonic nervous development [9]. They also play an important role in isoflurane-induced neurotoxicity; for instance, miR-214 protected against isoflurane-induced SH-SY5Y cell apoptosis through the PI3K/Akt pathway by targeting PTEN [10]. MiR-137 is a brain-enriched miRNA and plays a critical role in regulating the development of the proliferation and differentiation of neurons and the maturation of synapses [11]. MiR-137 is associated with neurodevelopment and thus affects dendrite morphogenesis, phenotypic maturation, and spinal development in adult hippocampal neurons by targeting MIB1 [12]. MiR-137 can also be coordinated with CDC42 to protect against ketamine-induced hippocampal neurodegeneration in rats [13]. However, to our knowledge, the effect of miR-137 on long-term isoflurane exposure has not yet been investigated. Given the important roles of miR-137 in neurons, it is interesting to elucidate whether isoflurane-induced neurotoxicity involves miR-137.

Dexmedetomidine (DEX) is a highly specific  $\alpha_2$ -adrenergic agonist. It has the characteristics of sedation, analgesia, anti-anxiety, and maintenance of hemodynamic stability. DEX has antioxidative stress, anti-inflammatory and antiapoptotic effects in various diseases, including LPS-induced acute lung injury [14] and postoperative cognitive dysfunction in aged mice [15]. DEX was also confirmed to reduce isoflurane-induced neuronal apoptosis and neurocognitive dysfunction in neonatal rats [16,17]. DEX could also reduce isoflurane-induced hippocampal neuron apoptosis in neonatal rats by regulating NR2A, NR2B and EAAT1 or the P13K/Akt pathway [18,19]. Furthermore, DEX could reduce a variety of cell or tissue damage by regulating the miRNAs and their target genes. For example, DEX attenuated hippocampal neuronal apoptosis and cognitive impairment by mediating the miR-129/Yap1/Jag1 axis in an Alzheimer's disease mouse model [20]. DEX could suppress LPS-induced neuroinflammation by upregulating miR-340 and inhibiting the NF- $\kappa$ B pathway in BV2 microglia [21]. However, the effect of DEX on miR-137 is still unknown. A previous study suggested that miR-137 could able to exert a tumor-suppressive effect on gastric cancer cells by targeting the 3' UTR of GSK-3 $\beta$  mRNA [22] and negatively regulates the protein levels of GSK-3 $\beta$  [23]. GSK-3 $\beta$  is ubiquitously expressed throughout the brain, most prominently in the cerebral cortex and hippocampus [24]. Evidence suggests that GSK-3 $\beta$  is a key activator of cell death in neuronal apoptosis [25]. For instance, miR-15b-5p could regulate neuronal apoptosis through the GSK-3 $\beta$ / $\beta$ -catenin signaling pathway [26]. However, in the adult hippocampal dentate gyrus, GSK-3 $\beta$  inhibitors increase neural stem cell proliferation, migration, and differentiation [27]. Moreover, exposure to clinically relevant concentrations of sevoflurane promoted mitochondrial fission and apoptosis in the mitochondria in the neonatal mouse hippocampus and in SKNSH cells by activating a GSK-3 $\beta$ /Drp1-dependent manner [28]. Isoflurane has also been reported to inhibit neural stem cell viability and proliferation and promote their apoptosis by increasing cleaved caspase-3 and downregulating GSK-3 $\beta$  [29]. In addition, we predicted that GSK-3 $\beta$  is one of a target gene of miR-137-3p by using the miRbase and TargetScan databases. Therefore, it is reasonable to assume that isoflurane-induced neuronal apoptosis involves the miR-137/GSK-3 $\beta$  pathway.

In this study, we hypothesized that isoflurane induces neuronal apoptosis via the miR-137/GSK-3 $\beta$  pathway and that DEX plays a protective role by negatively regulating the miR-137/GSK-3 $\beta$  pathway. For this, we established an isoflurane exposure model in Sprague–Dawley (SD) rats at an early age and a PC12 cell line to investigate the neuroprotective mechanism of DEX on isoflurane-induced neuroapoptosis. Our results contribute information toward understanding the neuroprotective mechanisms of DEX, which provide a new insight for further expanding the application of DEX in human and veterinary medicine.

## 2. Materials and Methods

### 2.1. Animals and treatments

Both sexes of postnatal day 7 (P7) SD rats, weighing 16–18 g were provided by Qingdao Daren Fortune Animal Technology Co. Ltd. All animals were housed with their mothers in polypropylene cages under a 12-h light-dark cycle at a constant room with 45%–55 % humidity, 24–26 °C and had free access to water and food.

We used 8 L P7 pups and chose four pups from each litter. Then the rats were randomly assigned into four groups (n = 8), including a control group (CON), a dexmedetomidine group (dexmedetomidine 25  $\mu$ g/kg, DEX), an isoflurane group (1.5 % isoflurane, Iso) and an isoflurane + DEX group (1.5 % isoflurane + DEX 25  $\mu$ g/kg, ISO + DEX). DEX (Hengrui Medicine Co., Ltd. Jiangsu, China) was received at 25  $\mu$ g/kg (refer to a previous study [30]) intraperitoneally before (30 min prior) exposure to 1.5 % isoflurane in the ISO + DEX group, and the same volume of DEX or normal saline was injected intraperitoneally in the DEX, CON and ISO groups. Isoflurane (Yipin pharmaceutical Co., Ltd., Hebei, China) was administered in an anesthesia chamber with 0 % anesthetic for the CON and DEX groups or 1.5 % anesthesia for the ISO and ISO + DEX groups mixed with 100 % oxygen using an agent-specific vaporizer (Matrx VMR, MIDMARK Corporation, Ohio, USA). A customized closed-circuit system was used to administered the agents, and soda lime was used to eliminate the carbon dioxide. After 6 h of exposure, the rats in each group were sacrificed and the brain were dissected out. Using forceps to dissect away the cerebral cortex carefully and expose the hippocampus. Then, the hippocampus was washed with physiological sodium chloride solution and harvested. Afterwards, the hippocampus was postfixed in 4 % paraformaldehyde saline or frozen in liquid nitrogen immediately and stored at –80 °C for gene and protein analysis.

## 2.2. Histopathological observation, terminal-deoxynucleotidyl transferase mediated dUTP nick-end labeling (TUNEL) and immunofluorescence (IF) analysis

The histological observation procedures were performed as described previously [31]. Briefly, the hippocampal specimens were fixed in 10 % neutral formalin for 24–48 h. After, the specimens were processed by paraffin wax and chopped into 5–6  $\mu\text{m}$  thickness. Then, the slices were stained with hematoxylin and eosin (HE, Wuhan Servicebio Technology Co., Ltd., Hubei, China) for histopathological observation, and the pathological scoring criteria was described as before [32]. TUNEL analysis was carried out using a one-step TUNEL apoptosis assay kit according to the manufacturer's instructions (Beyotime Biotechnology Co. Ltd., Jiangsu, China), and samples were observed under a fluorescence microscope (Nikon TE2000). The formula used for assessing the apoptosis rate was the number of TUNEL-positive nuclei (TUNEL specks)  $\times$  100 %/the total number of nuclei (DAPI). The numbers of positive cells in the hippocampal slices were counted in a randomly section at a high-magnification field ( $\times$  400) in three visual fields. For the IF assays, the slices were incubated with GSK-3 $\beta$  (1:400, Service-bio-Co., Ltd., Wuhan, China) antibody overnight at 4  $^{\circ}\text{C}$ , and then incubated with CY3 (1:500, Service-bio)-labeled IgG for 2–3 h. After they were mounted with DAPI (Service-bio), the sections were examined and acquired with a fluorescence microscope (Nikon TE2000).

## 2.3. Cell culture and treatment

PC12 cells are often used *in vitro* models of neurophysiological and neuropharmacological studies due to the general characteristics of neuroendocrine cells and are easier to subculture than primary neurons. Thus, PC12 cells with a high degree of differentiation (donated by the Department of Veterinary Surgery, Northeast Agricultural University) were cultured in Dulbecco's modified Eagle's medium (DMEM) containing 10 % fetal bovine serum in a humidified incubator containing 5 %  $\text{CO}_2$  at 37  $^{\circ}\text{C}$ . Before exposure to isoflurane, DEX cytotoxicity was measured using a cell counting kit-8 (CCK-8, Beyotime) and lactate dehydrogenase (LDH) cytotoxicity assay kit (Beyotime). Briefly,  $1 \times 10^4$  PC12 cells were seeded in 96-well plates until they reached the logarithmic phase and then cultured with a concentration gradient of DEX for 24 h. For the CCK-8 analysis, CCK-8 solution was added into each well at a final concentration of 10 %, and cells were subsequently incubated at 37  $^{\circ}\text{C}$  for 2 h. Then, the absorbance was measured at 450 nm using an automatic microplate reader (BioTek Epoch, Winooski, USA). For LDH analysis, the cell well was washed with PBS, and 150  $\mu\text{L}$  LDH solution was added and incubated for 1 h. After centrifugation at 500  $\times g$  for 5 min, 100  $\mu\text{L}$  LDH solution was transferred to a new 96-well plate to measure the absorbance at 490 nm using a microplate reader (BioTek Epoch).

To confirm the effect of DEX on isoflurane-induced neurotoxicity, PC12 cells were cultured in 6-well plates and grown to 70%–80 % confluence. Then, well plates were randomly assessed as the CON, DEX, ISO and ISO + DEX groups. The DEX, ISO + DEX and CON groups were pretreated (30 min prior) with 25  $\mu\text{g}/\text{mL}$  (obtained from the DEX cytotoxicity results) DEX or the same volume of PBS according to the cell cytotoxicity results. Then, the plates were exposed to 21 %  $\text{O}_2$  and 5 %  $\text{CO}_2$  with (ISO and ISO + DEX groups) or without (CON and DEX groups) 1.5 % isoflurane as described by Xie et al. for 6 h [33]. Then, the cells were cultured in DMEM with 10 % FBS in a humidified incubator containing 5 %  $\text{CO}_2$  at 37  $^{\circ}\text{C}$  until they grew to >90 % confluence and then harvested for further analysis.

## 2.4. Oligonucleotide transfection

The sequences of miR-137 negative control (NC, 5'-UUCUCCGAACGUGUCACGUTT-3'; 5'-ACGUGACACGUUCGGAGAATT-3'), mimics (5'-UUAUUGCUUAAGAAUACGCGUAG-3'; 5'-ACGCGUAUUCUUAAGCAAUAAUU-3'), inhibitor negative control (INC, 5'-CAGUACUUUUGUGUAGUACAA-3') and inhibitor (5'-CUACGCGUAUUCUUAAGCAAUAA-3'), were chemically synthesized by Gene Pharma Co., Ltd. (Shanghai, China). Then, the sequences were transfected into PC12 cells using Lipofectamine 3000 (3.0  $\mu\text{g}/\text{mL}$ , Invitrogen) in Opti-MEM (Gibco). Twenty-four hours later, the cells were incubated in DMEM with 10 % FBS for 12 h and then harvested for quantitative real-time PCR (qRT-PCR) and other analyses. According to the qRT-PCR results, both the final concentrations of miR-137 mimics and inhibitor were 150 nM.

## 2.5. Dual luciferase reporter assay

The miR-137 target GSK-3 $\beta$  3'UTR sequence was cloning into the pMIR-REPORT vector to construct the luciferase reporter. Briefly, the GSK-3 $\beta$  3'UTR oligonucleotides containing two tandem repeats of miR-137 were constructed as wild-type (WT) or mutant-type (MT) primers (Table 1). After annealed at 95  $^{\circ}\text{C}$  for 5 min, the oligonucleotides (synthesized by Tsingke Biotech Co., Ltd., Qingdao, China) were inserted into the *Hind* III and *Sac* I sites of the pMIR-REPORT vector and verified by direct sequencing (Tsingke). Then, the

**Table 1**  
The primer sequences of the wild-type (WT) or mutant-type (MT) GSK3- $\beta$  3'UTR.

Names	Primer sequences (5'-3', F: forward; R: reverse)
GSK-3 $\beta$ -WT-F	AAGCTTGTTTTTGAAGAAAATCGTTAATTCCTTGGAAAGGAGCTC
GSK-3 $\beta$ -WT-R	CCTTCCAAGGAATATTGCTTTTCTTCAAAAACA
GSK-3 $\beta$ -MT-F	AAGCTTGTTTTTGAAGAAAATCGTTAATTCCTTGGAAAGGAGCTC
GSK-3 $\beta$ -MT-R	CCTTCCAAGGAATTAACGATTTCTTCAAAAACA

cells were plated in a 24-well plate and cotransfected with 150 nM miR-137 mimics or 100 nM NC, 500 ng pMIR-REPORT comprising GSK-3 $\beta$  3'UTR, and 10 ng phRL-TK (Promega) using Lipofectamine 3000 reagent in Opti-MEM. The cells were harvested after 24 h of transfection and analyzed using a Dual-Luciferase Reporter Assay System (Vazyme Biotech Co., Ltd, Nanjing, China).

## 2.6. Total mRNA extraction and qRT-PCR assay

The TRIzol (Sangon) method was adopted to extract total RNA from hippocampal tissues and PC12 cells. Then, 1.0  $\mu$ g of total RNA was reverse-transcribed into cDNA with the Prime Script Reagent Kit with gDNA Eraser (Takara Biomedical Technology Co., Ltd., Beijing, China) and the miRcute Plus miRNA First-Strand cDNA Kit (Tiangen Biotech Co., Ltd., Beijing, China) according to the manufacturer's instructions. The expression of miR-137 and the mRNAs were measured using the SYBR Green method on a LightCycler 480 Detection System (Roche, Basel, Switzerland). The qRT-PCR reactions system and procedures were performed as described before [34]. The primers (Table 2) were designed by using Primer 6.0 and synthesized by Tsingke. Data were obtained using the  $2^{-\Delta\Delta Ct}$  method, and U6 and  $\beta$ -actin were used as internal controls for normalization. When the cycle number less than 35 (total 40 cycles), considering the result was cut-off for acceptance.

## 2.7. Western blot analysis

Total protein was extracted from hippocampal tissues and PC12 cells with cell lysis buffer for Western blotting and IP (Beyotime). Protein concentration was normalized by an enhanced BCA protein assay kit (Beyotime). The total proteins were separated by using 8%~12% sodium dodecyl sulfate-polyacrylamide gel electrophoresis. Then, the separated proteins were transferred to 0.22  $\mu$ m or 0.45  $\mu$ m PVDF membranes. After blocking with 5% skim milk, the membranes were incubated with diluted primary antibodies (Table 3) at 4  $^{\circ}$ C for 12 h. Following incubation with secondary antibodies conjugated to horseradish peroxidase for 1.5 h at room temperature, the signal of the membranes was measured by enhanced chemiluminescence (Wanleibio) using a Tanon 5200 imaging system (Shanghai, China).

## 2.8. Statistical analysis

GraphPad Prism 8.3.0 software (USA) was used for statistical analysis and figure generation. The data are presented as the means  $\pm$  standard deviations (SD). One/Two-way analysis of variance (ANOVA) with Tukey's post hoc test was used for analysis among multiple groups.  $P < 0.05$  was considered statistically significant.

## 3. Results

### 3.1. DEX attenuates isoflurane-induced hippocampal damage in developing rats

The morphological changes in the hippocampus in the different groups were stained using the HE method. As shown in Fig. 1, the neurons of the hippocampal CA1, CA3 and dentate gyrus (DG) regions in the CON group and DEX group (Fig. 1A–C) had full cell bodies and normal sizes and were arranged closely in a compact order. The cytoplasm of the neuron was clear, and the cell nuclei were round or elliptical. However, in the ISO group (Fig. 1B), the number of hippocampal neurons presented a wide space and irregular arrangement with pyknotic and dense nuclei, deep cytoplasm staining, nuclear chromatin fragmentation (apoptotic-like cells, black and red arrows), and inflammatory infiltration (yellow arrows). This suggested that exposure to isoflurane for 6 h in developing rats could induce hippocampal damage. Nevertheless, the neuronal cells in the ISO + DEX group (Fig. 1D) showed little disordered arrangement, dense nuclei, and inflammatory infiltration, which suggested that DEX attenuates isoflurane-induced hippocampal damage.

### 3.2. DEX alleviates isoflurane-induced neuronal apoptosis in the hippocampus of developing rats

To further export the effect of DEX on isoflurane-induced hippocampal damage in developing rats, the apoptosis rate of the

**Table 2**  
miR-137 and mRNA primer sequences used in this study.

Names	Forward sequences (5'-3')	Reverse sequences (5'-3')
miR-137	GCGCGCGCGGTTATTGCTTAAGAATA	General reverse primer
U6	CTCGCTTCGGCAGCACATATACT	General reverse primer
$\beta$ -actin	ACAGCTTACCACCACAGCT	GAGGAAGAGGATCGCGCAGT
GSK-3 $\beta$	CAATCGCACTGTGTAGCCGTCCTC	GGTGTCTCGCCCATTTGGTAG
$\beta$ -catenin	ACAAGCCACAGGACTACAAGAAACG	TCAGCAGTCTCATTCCAAGCCATTG
Caspase-3	GCGGTATTGAGACAGACAGTGAAC	GCGGTAGAGTAAGCATACAGGAAGTC
Caspase 9	CAAGAAGAGCGGTTCCYGGTACATC	CAGCATTGGCGACCCTGAGAAG
Bax	GCGAGTGCTCAGGCGAATTGG	AGTCTGTATCCACATCAGCAATCATCC
Bcl-2	GGTGGTGGAGAACTCTCA	CATCTCCCTGTTGACGCTCT

**Table 3**  
The primary antibodies used in the present study.

Antibodies Names	Dilution multiple	Item No.	Manufacturers (Anti-rabbit)
GAPDH	1:3000	GB15004	Wuhan Servicebio Co., Ltd., Wuhan, China
$\beta$ -catenin	1:1000	bs-1165R	Bioss Technology Co. Ltd., Beijing, China
Caspase-9	1:1000	bs-20773R	Bioss Technology Co. Ltd., Beijing, China
Caspase-3	1:1000	bs-0081R	Bioss Technology Co. Ltd., Beijing, China
Bcl-2	1:500	WL01556	Wanleibio Co. Ltd., Shenyang, China
Cleaved-caspase-3	1:500	WL01992	Wanleibio Co., Ltd., Shenyang, China
Cleaved-caspase-9	1:500	WL01838	Wanleibio Co., Ltd., Shenyang, China
GSK-3 $\beta$	1:1000	GB11099	Servicebio Co., Ltd., Wuhan, China
Bax	1:1000	GB154122	Servicebio Co., Ltd., Wuhan, China

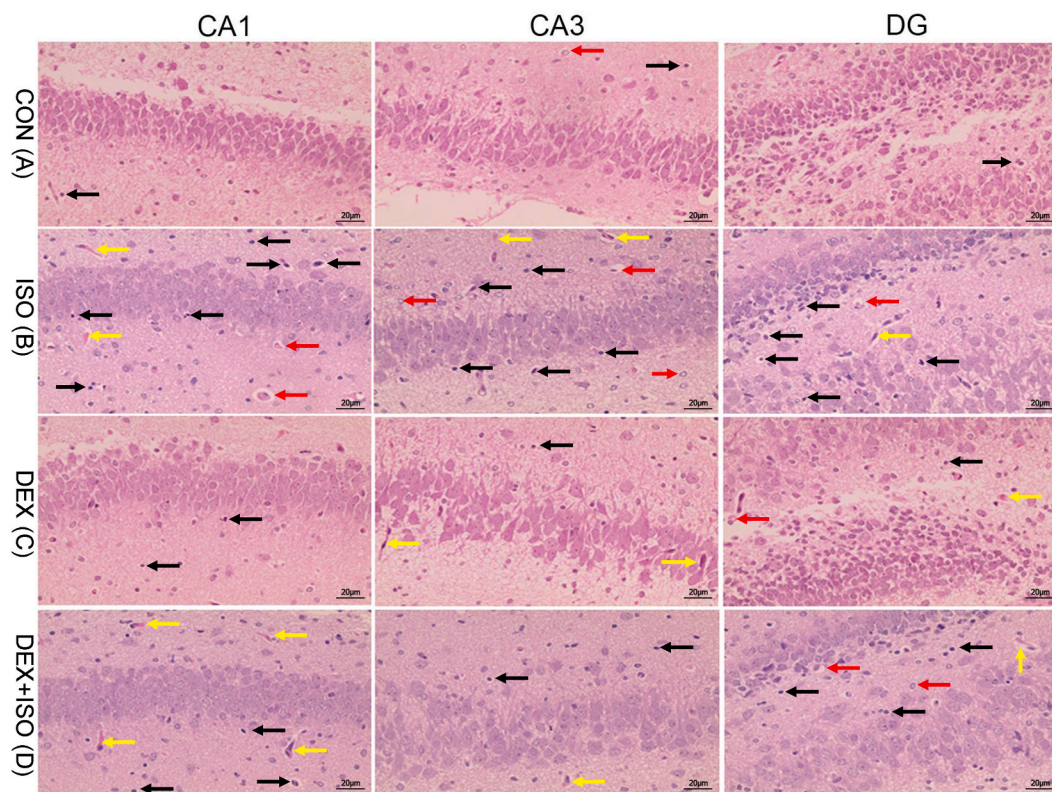


**Fig. 1.** Effects of DEX on isoflurane-induced hippocampal damage in developing rats. Histological examination of hematoxylin and eosin staining of the hippocampal CA1, CA3 and dentate gyrus (DG) regions in P7 SD rats ( $n = 3$ ). The histological results showed obvious nuclear solidification (black arrows), some vacuolization (red arrows), and some inflammatory infiltration (yellow arrows) in the CA1, CA3 and DG of the hippocampus in the ISO group (B, ++, histopathology in 20–60 % of the fields). Less nuclear solidification and vacuolization were observed in the CON (A), DEX (C) and CON + DEX (D) groups (-, histopathology <10 % of the fields). Scale bar = 20  $\mu$ m in each group. P7 SD rats, postnatal day 7 Sprague–Dawley rats.

hippocampus was measured using the TUNEL method. We found that the number of TUNEL-positive cells (green fluorescence) in the ISO group was higher than that in the other groups (Fig. 2A). Quantitative analysis results suggested that the TUNEL-positive rate in the ISO group was significantly higher than that in the CON ( $P < 0.01$ ) and DEX ( $P < 0.01$ ) groups. However, the apoptosis rate in the ISO + DEX group was significantly decreased compared with that in the ISO group ( $P < 0.05$ ) (Fig. 2B), even though it was still higher than that in the CON ( $P < 0.01$ ) and DEX ( $P < 0.05$ ) groups.

Next, we assessed the apoptosis-related genes expression in the hippocampus. The results showed that ISO significantly upregulated the apoptosis-related genes Bax ( $P < 0.05$ ), caspase-9 ( $P < 0.01$ ) and caspase-3 ( $P < 0.05$ ) compared to the CON and DEX groups, while significantly downregulated the expression of Bcl-2 ( $P < 0.01$ ) (Fig. 2C–F). However, pretreatment with DEX (DEX + ISO group) significantly decreased the expression of Bax ( $P < 0.05$ ), caspase-9 ( $P < 0.01$ ) and caspase-3 ( $P < 0.01$ ), and significantly increased the Bcl-2 ( $P < 0.05$ ) expression compared with the ISO group. In addition, the relative protein expression (Fig. 2G–K) of apoptosis-related

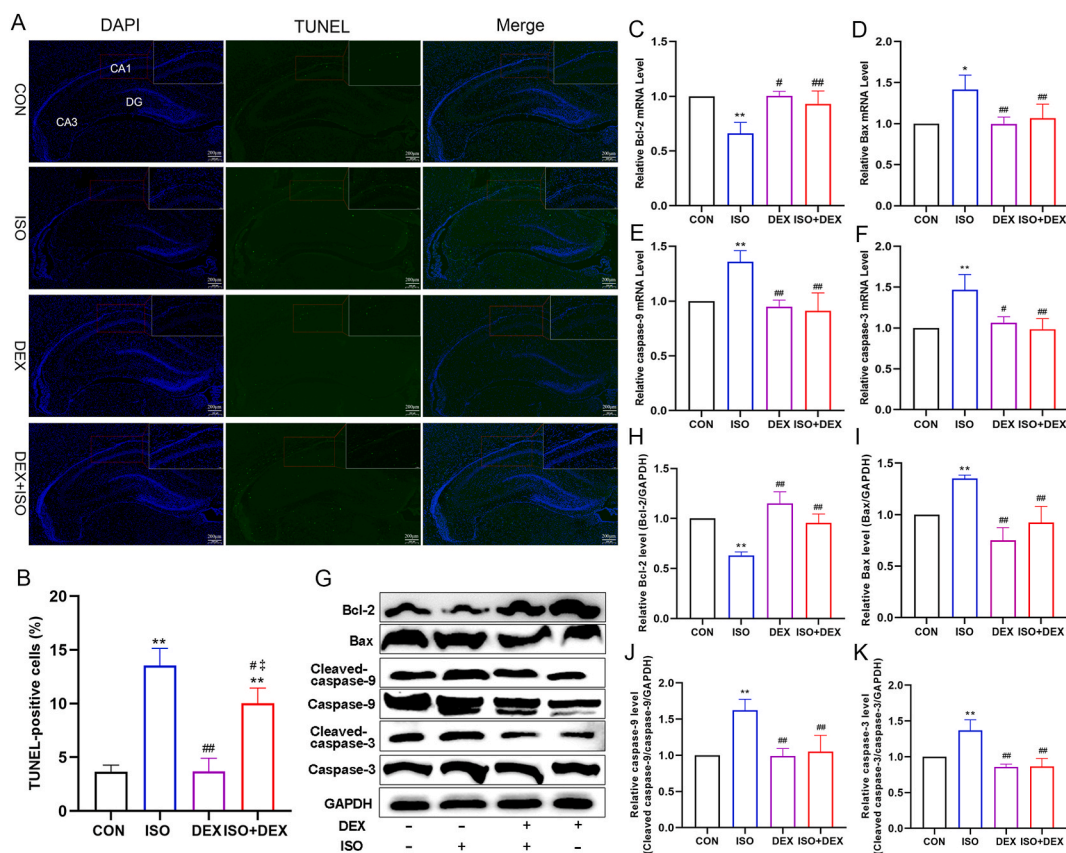


**Fig. 2.** DEX alleviates isoflurane-induced neuronal apoptosis in the hippocampus. The apoptosis index was measured by TUNEL (A) and quantitatively analyzed using ImageJ (B) ( $n = 3$ ). The formula used for assessing the apoptosis rate was the number of TUNEL-positive nuclei (TUNEL specks)  $\times 100\%$  / the total number of nuclei (DAPI). The TUNEL-positive cells were stained green, and the bars represent 100  $\mu\text{m}$ . The relative mRNA (C–F) and protein (G–K) expression levels of apoptosis-related genes in the hippocampus were measured using qRT-PCR and Western blot ( $n = 6$ ). Data are expressed as the mean  $\pm$  SD. \* $P < 0.05$ , \*\* $P < 0.01$  exhibited a significant difference compared to the CON group, # $P < 0.05$ , ## $P < 0.01$  exhibited a significant difference compared to the ISO group.

genes was consistent with the expression of their mRNAs. This result suggested that DEX alleviates isoflurane-induced neuronal apoptosis in the hippocampus.

### 3.3. DEX increases miR-137 and decreases GSK-3 $\beta$ in the hippocampus of rats

Due to the neurodevelopmental and neuroprotective effects of miR-137, we next investigated the expression of miR-137 in the hippocampus to confirm whether isoflurane-induced neurotoxicity involves miR-137. As shown in Fig. 3A, compared with that in the CON group, the expression of miR-137 in the ISO group was decreased significantly ( $P < 0.01$ ) but was not significantly different in the ISO + DEX ( $P > 0.05$ ) group. Interestingly, the expression of miR-137 in the DEX group was significantly increased ( $P < 0.01$ ) compared with that in the other groups. GSK3- $\beta$  is a target gene of miR-137 and is ubiquitously expressed in the brain, where it is a key activator of cell death. Then, we further investigated the expression of GSK3- $\beta$ . The immunofluorescence histochemistry results showed that the expression of GSK3- $\beta$  (red fluorescence) in the ISO group was increased compared with that in the other groups (Fig. 3B, magnified results show the CA1 region of the hippocampus). Quantitative analysis (Fig. 3C) suggested that the average gray value of GSK3- $\beta$  in the ISO group was significantly increased compared with that in the CON ( $P < 0.05$ ) and DEX ( $P < 0.01$ ) groups. However, the expression of GSK3- $\beta$  in the ISO + DEX group was significantly decreased ( $P < 0.05$ ) compared with that in the ISO group. Gene expression analysis also showed that GSK3- $\beta$  in the ISO group was increased significantly (Fig. 3D,  $P < 0.01$ ) but decreased significantly ( $P < 0.01$ ) in the DEX group compared with the CON group. The GSK3- $\beta$  level in the ISO + DEX group was decreased significantly ( $P < 0.05$ ) compared to that in the ISO group but was not significantly different ( $P > 0.05$ ) from that in the CON group. Furthermore, the relative GSK3- $\beta$  protein level also presented a similar result as its mRNA level (Fig. 3E and F). These results suggested that DEX increased miR-137 and decreased GSK3- $\beta$  in the hippocampus.

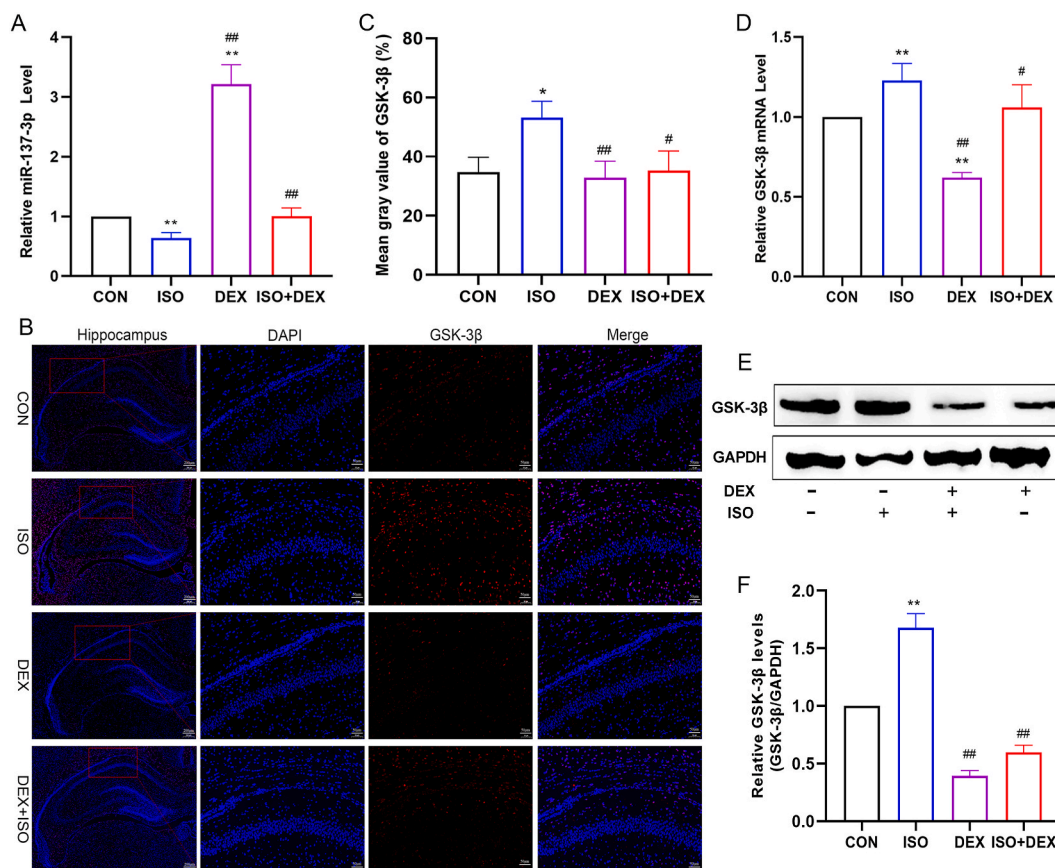


**Fig. 3.** DEX increased miR-137 and decreased GSK-3 $\beta$  in the hippocampus. The expression of miR-15a (A) was measured by qRT-PCR, and GSK-3 $\beta$  was measured by immunofluorescence (B, C) ( $n = 3$ ), qRT-PCR (D) and WB (E, F) ( $n = 6$ ). GSK-3 $\beta$  immunofluorescence was labeled with CY-3 (red) and quantitatively analyzed using ImageJ. The plotting scale bars represent 100  $\mu\text{m}$ , and the magnified CA1 region of the hippocampus is shown at 20  $\mu\text{m}$ . Data are expressed as the mean  $\pm$  SD. \* $P < 0.05$ , \*\* $P < 0.01$  exhibited a significant difference compared to the CON group, # $P < 0.05$ , ### $P < 0.01$  exhibited a significant difference compared to the ISO group.

### 3.4. DEX alleviates isoflurane exposure-induced PC12 apoptosis

To further explore the effect of miR-137 on neuronal apoptosis, we used the P12 cell line to establish the isoflurane exposure model and miR-137 knockdown/overexpression expression model, as PC12 cells have general characteristics of neuroendocrine cells and are frequently used as the model *in vitro* for neurodegenerative diseases [35]. First, we used the CCK-8 method to confirm that the optimal stimulatory concentration of DEX on PC12 cells probably ranged from 10 to 25  $\mu\text{g}/\text{mL}$  because DEX at these concentrations had little effect on cell activity (Fig. 4A). Second, we chose three different concentrations to assess the effect of ISO on PC12 cell activity. As shown in Fig. 4B and C, the addition of 25  $\mu\text{g}/\text{mL}$  DEX (ISO+25  $\mu\text{g}/\text{mL}$  DEX) to 10 % DMEM significantly ( $P < 0.01$ ) alleviated isoflurane exposure (ISO)-induced cell toxicity. In addition, pretreatment with 20~25  $\mu\text{g}/\text{mL}$  DEX for 30 min significantly decreased ( $P < 0.01$ ) the release of LDH caused by isoflurane exposure (Fig. 4C). According to this result, we suggested that DEX could protect against isoflurane-induced PC12 cell injury, and 25  $\mu\text{g}/\text{mL}$  DEX was used in our next *in vitro* experiments. Consequently, we investigated the effect of DEX on isoflurane-induced PC12 apoptosis. The apoptosis-related gene results suggested that Bax ( $P < 0.01$ ), caspase-3 ( $P < 0.01$ ) and caspase-9 ( $P < 0.05$ ) in the ISO group were significantly upregulated compared to those in the CON group, while the expression of Bcl-2 ( $P < 0.05$ ) was significantly downregulated (Fig. 4D). However, the expression of Bax ( $P < 0.05$ ), caspase-3 ( $P < 0.01$ ) and caspase-9 ( $P < 0.05$ ) in the ISO + DEX group was significantly decreased, but the expression of Bcl-2 was significantly increased ( $P < 0.05$ ) compared with that in the ISO group. In addition, the relative protein expression of apoptosis-related genes was consistent with the expression of their mRNAs (Fig. 4E and F). This result suggested that dexmedetomidine alleviates isoflurane exposure-induced PC12 apoptosis.

### 3.5. Dexmedetomidine increases miR-137 and decreases GSK-3 $\beta$ in PC12 cells

Next, we examined the expression of miR-137 and GSK-3 $\beta$  in PC12 cells after isoflurane exposure. As shown in Fig. 5A, the relative miR-137 level in the ISO group was significantly lower than that in the other groups ( $P < 0.05$ ). Meanwhile, the expression of miR-137

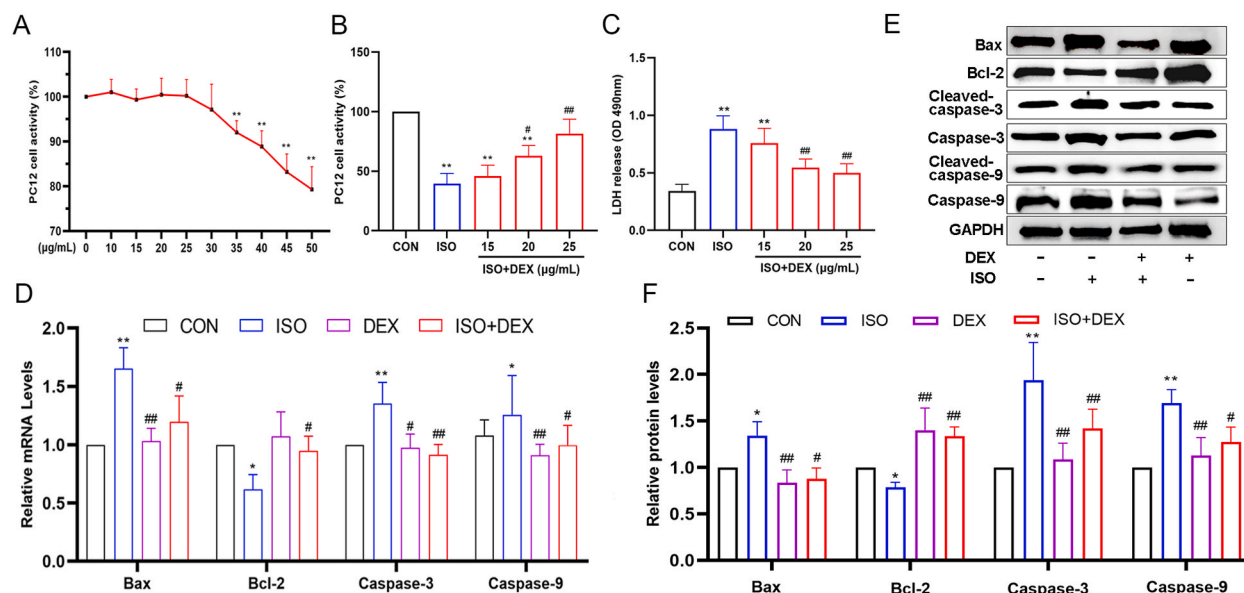


**Fig. 4.** Dexmedetomidine alleviated isoflurane exposure-induced PC12 apoptosis. The effect of different concentrations of DEX on PC12 cell viability (A) was measured using the CCK-8 method, and then three candidate concentrations of DEX were chosen to assess its effects on PC12 cell viability (B) and LDH release (C) ( $n = 3$ ). A concentration of 25  $\mu\text{g/mL}$  DEX was considered to be the most appropriate concentration for *in vitro* experiments. The relative mRNA (D) and protein (E, F) expression of apoptosis-related genes in PC12 cells was measured using qRT-PCR and WB ( $n = 3$ ). Data are expressed as the mean  $\pm$  SD ( $n = 3$ ). \* $P < 0.05$ , \*\* $P < 0.01$  exhibited a significant difference compared to the CON group, # $P < 0.05$ , ## $P < 0.01$  exhibited a significant difference compared to the ISO group.

in the DEX group was significantly higher than that in the ISO ( $P < 0.01$ ) and CON ( $P < 0.05$ ) groups. The GSK-3 $\beta$  mRNA and protein levels were significantly higher in the ISO group than in the CON ( $P < 0.05$  and  $P < 0.01$ , respectively) and DEX (both  $P < 0.01$ ) groups (Fig. 5B–D); however, in the ISO + DEX group, the GSK-3 $\beta$  mRNA ( $P < 0.05$ ) and protein ( $P < 0.01$ ) levels were significantly downregulated compared with those in the ISO group. These results were similar to the results in isoflurane-induced hippocampal damage in developing rats, which suggested that miR-137 and GSK-3 $\beta$  have a negative regulatory relationship.

To investigate the negative relationship between miR-137 and GSK-3 $\beta$ , we established miR-137 overexpression and knockdown models in PC12 cells. As shown in Fig. 5E, after transfection for 24 h, compared with the CON and NC group, the miR-137 level was significantly increased in the mimics group, whereas it was decreased significantly in the inhibitor group. According to the results, we confirmed that both the concentrations of the miR-137 mimics and inhibitor were 150 nM for subsequent experiments. Furthermore, miR-137 mimics significantly downregulated GSK-3 $\beta$  mRNA ( $P < 0.01$ ) and protein ( $P < 0.05$ ) levels, whereas miR-137 inhibitor significantly upregulated them (both  $P < 0.01$ ) (Fig. 5F–H), which suggested that miR-137 and GSK-3 $\beta$  have a negative relationship.

To confirm the relationship of miR-137 and GSK-3 $\beta$ , the TargetScan tool was used to predict their target relationship (Fig. 5I). The WT or MT 3'UTR of GSK-3 $\beta$  in the pMIR-REPORT plasmids (Fig. 5J) was constructed and cotransfected into PC12 cells with miR-137 mimics or NC. The results showed that miR-137 mimics significantly decreased the luciferase activity of the GSK-3 $\beta$ -WT 3'UTR ( $P < 0.01$ ) but had little effect on the GSK-3 $\beta$ -MT group (Fig. 5K). This result confirms that miR-137 has a target relationship with GSK-3 $\beta$ .

### 3.6. miR-137 suppresses PC12 cell apoptosis via the GSK-3 $\beta$ / $\beta$ -catenin pathway

GSK-3 $\beta$  inhibition rescues cell death in neuronal and nonneuronal cell lines by increasing  $\beta$ -catenin and its associated transcriptional pathway [36]. Then, we examined the expression of  $\beta$ -catenin in the hippocampus and PC12 cells exposed to isoflurane. As shown in Fig. 6A–E, in the ISO group, the relative  $\beta$ -catenin level was significantly lower than that in the CON group in the hippocampus ( $P < 0.05$ ) and PC12 cells ( $P < 0.01$ ). Compared with the ISO group,  $\beta$ -catenin mRNA (both  $P < 0.05$ ) was significantly increased in the ISO + DEX group. And the protein levels of  $\beta$ -catenin showed a similar trend as the  $\beta$ -catenin mRNA levels. To reveal the effect of miR-137 overexpression and knockdown on the GSK-3 $\beta$ / $\beta$ -catenin pathway,  $\beta$ -catenin mRNA ( $P < 0.05$ ) and protein were examined. As shown in Fig. 6F and G, the  $\beta$ -catenin mRNA and protein levels were significantly up-regulated (both  $P < 0.05$ ) in the miR-137 mimics group, while they were significantly down-regulated (both  $P < 0.05$ ) in the miR-137 inhibitor group. miR-137 could inhibit GSK-3 $\beta$  to upregulate  $\beta$ -catenin levels. Meanwhile, we explored the relationship of miR-137 with cell apoptosis, and we examined the expression of apoptosis-related genes and proteins. The results suggested that miR-137 mimics significantly suppressed the apoptosis-related genes Bax ( $P < 0.01$ ), caspase-3 ( $P < 0.01$ ) and caspase-9 ( $P < 0.05$ ) but increased the expression of Bcl-2 ( $P < 0.01$ ) comparing with the CON group; however, the opposite results were found in the inhibitor group (Fig. 6H). Apoptosis-related protein levels showed the same trend as apoptosis-related genes (Fig. 6I and J), indicating that miR-137 could inhibit PC12 apoptosis.

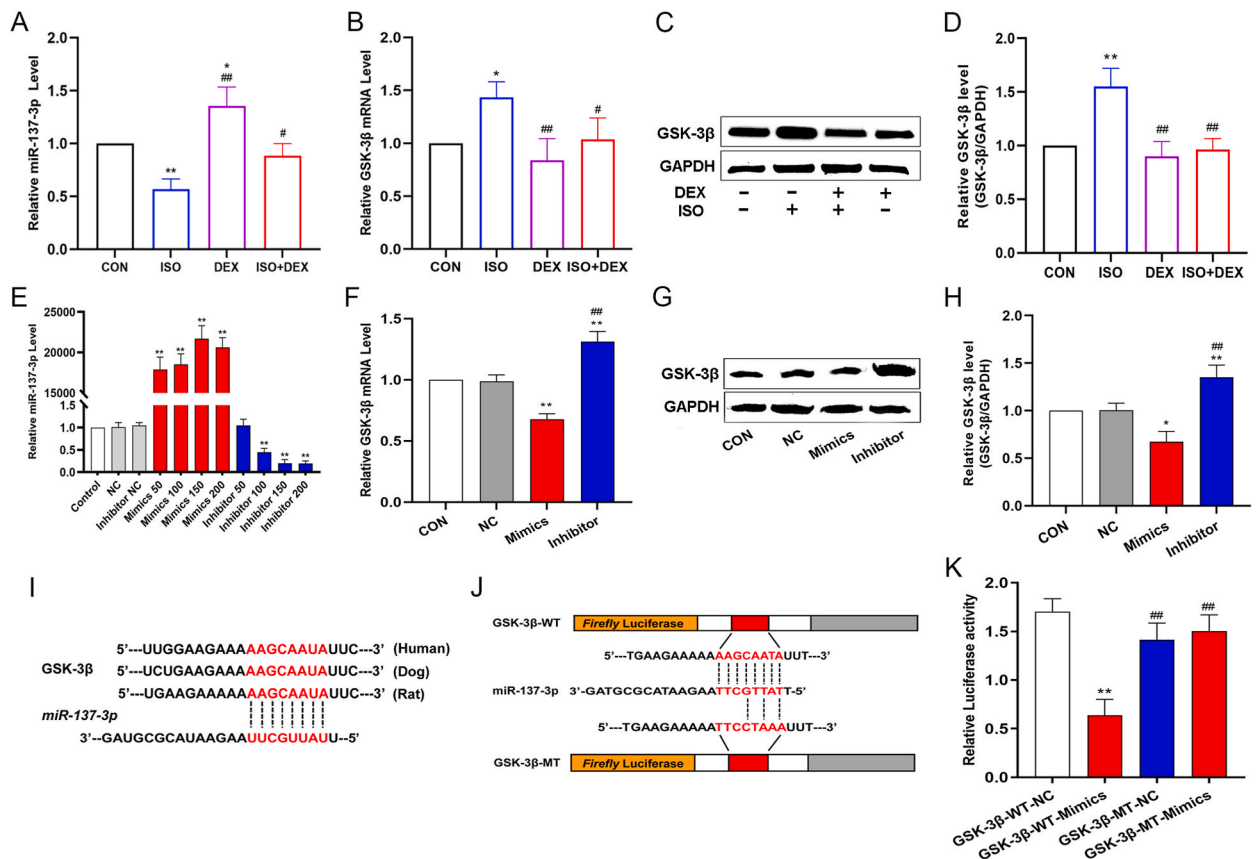


**Fig. 5.** GSK-3 $\beta$  was a negative-regulated gene of miR-137. Effects of DEX on miR-137 (A) and GSK-3 $\beta$  (B–D) in isoflurane exposure-induced PC12 cell apoptosis model. The transfection efficiency of miR-137 mimics and inhibitor (E) in PC12 cells was estimated, and both 150 nM mimics and inhibitor concentrations were used in this study. The effect of miR-137 on GSK-3 $\beta$  in PC12 cells was measured using qRT-PCR (F) and Western blot (G–H). The negative-regulated relationship between miR-137 and GSK-3 $\beta$  was predicted by TargetScan (I). The sequences of wild type (WT) and mutant type (MT) GSK-3 $\beta$  3'UTR were cloned into pMIR-REPORT plasmids, and the binding sites are marked in red (J). Their relationship was measured by dual luciferase reporter assay (K). Relative firefly luciferase expression was normalized to Renilla luciferase. Data are shown as the mean  $\pm$  SD (n = 3). \*\* $P$  < 0.01 presented a significant difference compared to the CON or GSK-3 $\beta$ -WT-NC group. ## $P$  < 0.01 indicates a significant difference compared to the ISO or miR-137 mimics or GSK-3 $\beta$ -WT-mimics group. UTR, untranslated region.

#### 4. Discussion

Long-term isoflurane inhalation has been reported to induce neurotoxicity and increase nerve cell death in young animals [37], as they are susceptible to acute neural injuries in this growth period. In this experiment, we confirmed that isoflurane induced pathological changes and caused apoptosis in the hippocampus, whereas DEX reduced isoflurane-induced neuronal apoptosis, which was similar to previous studies [16,17]. Bahmad's review suggested that microRNA was related to the mechanisms of anesthesia-induced neurotoxicity, cognitive decline and memory impairment [38]. Thus, it would be meaningful to investigate whether miRNA is beneficial against the neurotoxic effects of anesthetics.

MiR-137 has important implications in neurodevelopmental processes and in the biological regulation of cancer [11]. For instance, a study has shown that miR-137 protects neurons from oxygen and glucose deprivation-induced neuron damage [39]. Furthermore, downregulating miR-137 aggravated ketamine-induced hippocampal neuron apoptosis [13]. Therefore, it is interesting to elucidate the effect of miR-137 on isoflurane-induced neurotoxicity. In this study, we found that miR-137 was decreased in the hippocampus after isoflurane exposure for 6 h (ISO group), indicating that miR-137 was involved in isoflurane-induced nerve damage. However, DEX increased the miR-137 level in the DEX and DEX + ISO treatment groups in the hippocampus. In connection with the reduced apoptosis of hippocampal neurons in the DEX + ISO group, the neuroprotective mechanism of DEX may involve upregulating miR-137.

GSK-3 $\beta$ , one of the target genes of miR-137, is ubiquitously expressed throughout the brain and is most prominently expressed in the cerebral cortex and hippocampus. In this study, we found that GSK-3 $\beta$  was increased in isoflurane-induced hippocampal neuronal apoptosis, which is in line with previous studies [40,41]. Moreover, DEX attenuated the isoflurane-induced increase in GSK-3 $\beta$  in the hippocampus. This result suggested that the neuroprotective mechanism of DEX may involve miR-137-mediated GSK-3 $\beta$ . To study the relationship of miR-137 and GSK-3 $\beta$ , we first used the TargetScan tool to predict their negative relationship, and the results suggested that miR-137 could directly target GSK-3 $\beta$ . Meanwhile, we also observed their negative relationship in another study, such as in a

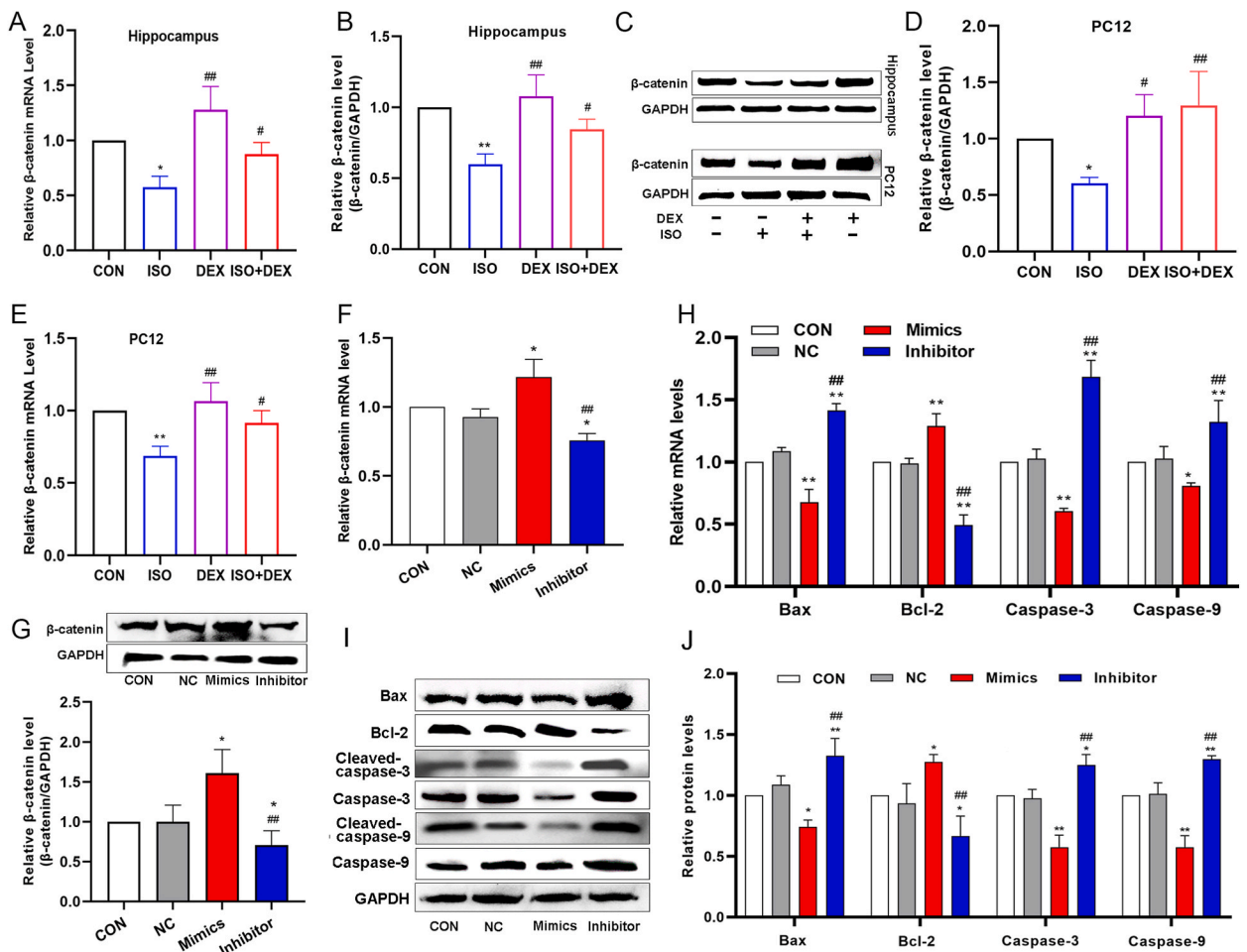


**Fig. 6.** miR-137 suppressed the GSK-3 $\beta$ / $\beta$ -catenin pathway and DEX induced PC12 cell apoptosis. Relative expression of  $\beta$ -catenin was measured in isoflurane-induced hippocampus (A–C) and PC12 (C–E) injury models, as well as in miR-137 overexpression and knockdown PC12 model (F–G) using qRT-PCR and Western blot, respectively. The relative expression of apoptosis genes was measured using qRT-PCR (H) and Western blot (I–J) in the miR-137 overexpression and knockdown PC12 model. Data are shown as the mean  $\pm$  SD (n = 3). \* $P$  < 0.05, \*\* $P$  < 0.01 presented a significant difference compared to the CON group. # $P$  < 0.05, ## $P$  < 0.01 indicates a significant difference compared to the ISO or miR-137 mimics group.

mouse neuroblastoma cell line [23]. Second, we confirmed their negative regulatory relationship using a dual-luciferase reporter assay in the PC12 cell line, as it is often used in neurophysiological and neuropharmacological studies *in vitro*. In addition, we established an isoflurane exposure model in PC12 cells and assessed the protective effect of DEX in isoflurane-exposed PC12 cells. Before the addition of DEX *in vitro*, the dose of DEX was considered, although several studies have shown that DEX is nontoxic [42]. According to the cell viability and LDH cytotoxicity assays, 25  $\mu$ g/mL was recommended as the optimum concentration. The *in vitro* results suggested that DEX alleviates isoflurane exposure-induced PC12 apoptosis, which was generally consistent with the *in vivo* study and previous research [16,43]. In addition, we found that DEX upregulated miR-137 and downregulated GSK-3 $\beta$  in an isoflurane-induced PC12 injury model, which also reflects the target relationship of miR-137 and GSK-3 $\beta$ .

A study suggested that a GSK-3 $\beta$  inhibitor prevented cardiomyocyte apoptosis by abrogating the enhanced ratio of cleaved caspase-3/caspase-3 and decreased Bcl-2 expression [44]. Upregulation of GSK-3 $\beta$  not only induces a neuroinflammatory response but also causes neurodegenerative diseases and neuronal apoptosis [45,46]. GSK-3 $\beta$  is known as an inhibitor of  $\beta$ -catenin, which can decrease  $\beta$ -catenin and depress nerve growth factor-induced differentiation [47]. Losing  $\beta$ -catenin can induce embryonic liver apoptosis [48], and a review also suggested that downregulating  $\beta$ -catenin may underlie the mechanism of neuronal death in Alzheimer's disease and Down syndrome [49]. Combined with this evidence, we supported that GSK-3 $\beta$  was upregulated and  $\beta$ -catenin was downregulated in isoflurane-induced apoptosis *in vivo* and *in vitro*, which was consistent with our hypothesis. Moreover, we found that DEX-mediated isoflurane exposure induced an increase in GSK-3 $\beta$  and a decrease in  $\beta$ -catenin. These results suggest that the GSK-3 $\beta$ / $\beta$ -catenin pathway at least partly participates in the neuroprotective mechanism of dexmedetomidine.

To investigate the effect of miR-137 on the GSK-3 $\beta$ / $\beta$ -catenin pathway, we established miR-137 overexpression and knockdown models in PC12 cells. We found that overexpressing miR-137 could inhibit GSK-3 $\beta$  and increase  $\beta$ -catenin, whereas knocking down

miR-137 upregulated GSK-3 $\beta$  and downregulated  $\beta$ -catenin. We also found that overexpression of miR-137 increased Bax, caspase-9 and caspase-3 expression and decreased Bcl-2 expression, thus promoting PC12 cell apoptosis; however, knockdown of miR-137 produced the opposite results. Upregulating miR-137 could effectively inhibit propofol-induced cell apoptosis and protect cognitive dysfunction [50], and similar results were also found in prostate cancer and esophageal squamous cell carcinoma [51,52]. However, in this study we did not analysis the neuroprotective of DEX on isoflurane-induced cognitive dysfunction when these rats adults, and as well as the miR-137 and GSK-3 $\beta$ . We will further explore their crosstalk mechanism in our next study.

## 5. Conclusions

In this study, we demonstrated that miR-137 was involved in isoflurane-induced hippocampal neuron apoptosis in developing rats. We declared that DEX could upregulate miR-137 and then attenuate isoflurane-induced neuroapoptosis through the GSK-3 $\beta$ / $\beta$ -catenin pathway in the developing rat hippocampus.

## Ethics statement

This study was reviewed and approved by the Animal Ethics Committee of Qingdao Agricultural University with the approval number: 2019-021, dated 03/21/2019.

## Data availability statement

The data associated with this study have not been deposited into a publicly available repository. The original data used to support the findings of this study will be made available on request from the corresponding author.

## CRedit authorship contribution statement

**Xueyuan Hu:** Writing – review & editing, Software, Funding acquisition, Formal analysis, Conceptualization. **Zihan Sun:** Writing – original draft, Methodology, Data curation. **Wenjing Wang:** Writing – original draft, Methodology, Data curation. **Gong Xiao:** Writing – review & editing, Software, Methodology. **Quanlin Yu:** Writing – review & editing, Methodology, Data curation. **Liang Chi:** Writing – review & editing, Data curation. **Huanqi Liu:** Writing – review & editing, Supervision, Conceptualization.

## Declaration of Competing interest

The authors declare that they have no known competing financial interests or personal relationships that could have appeared to influence the work reported in this paper.

## Acknowledgements

We would like to thank the funding of the project of Shandong Natural Science Foundation (ZR2022QC157), Shandong Modern Agricultural Technology and Industry System Innovation Team (SDAIT-09-05), and Doctoral Fund project of Qingdao Agricultural University (6651122010). We also would like to thank Shandong Key Laboratory for Preventive Veterinary Medicine at the College of Veterinary Medicine, Qingdao Agricultural University.

## Appendix A. Supplementary data

Supplementary data to this article can be found online at <https://doi.org/10.1016/j.heliyon.2024.e31372>.

## References

- [1] H. Wei, G. Liang, H. Yang, Isoflurane preconditioning inhibited isoflurane-induced neurotoxicity, *Neurosci. Lett.* 425 (1) (2007) 59–62.
- [2] V. Jevtovic-Todorovic, R.E. Hartman, Y. Izumi, et al., Early exposure to common anesthetic agents causes Widespread neurodegeneration in the developing rat brain and persistent learning deficits, *J. Neurosci.* 23 (3) (2003) 876–882.
- [3] Arvind Palanisamy, Mark G. Baxter, Pamela K. Keel, et al., Rats exposed to isoflurane in utero during early gestation are behaviorally abnormal as adults, *Anesthesiology* 114 (3) (2011) 521–528.
- [4] Zhongcong Xie, Deborah J. Culley, Yuanlin Dong, et al., The common inhalation anesthetic isoflurane induces caspase activation and increases amyloid beta-protein level in vivo, *Ann. Neurol.* 64 (6) (2008) 618–627.
- [5] Mary Ellen McCann, S.G. Soriano, Does general anesthesia affect neurodevelopment in infants and children? *Br. Med. J.* 367 (2019) l6459.
- [6] V. Jevtovic-Todorovic, A.R. Absalom, K. Blomgren, et al., Anaesthetic neurotoxicity and neuroplasticity: an expert group report and statement based on the BJA Salzburg Seminar, *Br. J. Anaesth.* 111 (2) (2013) 143–151.
- [7] Wenqian Yang, Qulian Guo, Jingyi Li, et al., microRNA-124 attenuates isoflurane-induced neurological deficits in neonatal rats via binding to EGR1, *J. Cell. Physiol.* 234 (12) (2019) 23017–23032.
- [8] R.C. Lee, R.L. Feinbaum, V. Ambrost, The *C. elegans* heterochronic gene *lin-4* encodes small RNAs with antisense complementarity to *lin-14*, *Cell* 75 (1993) 843–854.

- [9] Jaya Visvanathan, Seunghee Lee, Bora Lee, et al., The microRNA miR-124 antagonizes the anti-neural REST/SCP1 pathway during embryonic CNS development, *Gene Dev.* 21 (7) (2007) 744–749.
- [10] Qiaoling Wu, You Shang, Tu Shen, et al., Neuroprotection of miR-214 against isoflurane-induced neurotoxicity involves the PTEN/PI3K/Akt pathway in human neuroblastoma cell line SH-SY5Y, *Arch. Biochem. Biophys.* 678 (2019) 108181.
- [11] E. Mahmoudi, M.J. Cairns, MiR-137: an important player in neural development and neoplastic transformation, *Mol. Psychiatr.* 22 (1) (2017) 44–55.
- [12] Richard D. Smrt, Keith E. Szulwach, Rebecca L. Pfeiffer, et al., MicroRNA miR-137 regulates neuronal maturation by targeting ubiquitin ligase mind bomb-1, *Stem Cell.* 28 (6) (2010) 1060–1070.
- [13] C. Huang, X. Zhang, J. Zheng, et al., Upregulation of miR-137 protects anesthesia-induced hippocampal neurodegeneration, *Int. J. Clin. Exp. Pathol.* 7 (8) (2014) 5000–5007.
- [14] C. Fu, X. Dai, Y. Yang, et al., Dexmedetomidine attenuates lipopolysaccharide-induced acute lung injury by inhibiting oxidative stress, mitochondrial dysfunction and apoptosis in rats, *Mol. Med. Rep.* 15 (1) (2016) 131.
- [15] X.L. Qian, W. Zhang, M.Z. Liu, et al., Dexmedetomidine improves early postoperative cognitive dysfunction in aged mice, *Eur. J. Pharmacol.* 746 (2015) 206–212.
- [16] Robert D. Sanders, Jing Xu, Shu Yi, et al., Dexmedetomidine attenuates isoflurane-induced neurocognitive impairment in neonatal rats, *Anesthesiology* 110 (2009) 1077–1085.
- [17] R.D. Sanders, P. Sun, S. Patel, et al., Dexmedetomidine provides cortical neuroprotection: impact on anaesthetic-induced neuroapoptosis in the rat developing brain, *Acta Anaesthesiol. Scand.* 54 (6) (2010) 710–716.
- [18] Yujuan Li, Minting Zeng, Weiqiang Chen, et al., Dexmedetomidine reduces isoflurane-induced neuroapoptosis partly by preserving PI3K/Akt pathway in the hippocampus of neonatal rats, *PLoS One* 9 (4) (2014) e93639.
- [19] Xue Wang, Yangyang Shan, Zhiyin Tang, et al., Neuroprotective effects of dexmedetomidine against isoflurane-induced neuronal injury via glutamate regulation in neonatal rats, *Drug Des. Dev. Ther.* 13 (2019) 153–160.
- [20] Weiyang Sun, Jun Zhao, C. Li, Dexmedetomidine provides protection against hippocampal neuron apoptosis and cognitive impairment in mice with Alzheimer's disease by mediating the miR-129/YAP1/JAG1 Axis, *Mol. Neurobiol.* 57 (12) (2020) 5044–5055.
- [21] Yang Bao, Yijun Zhu, Guangbao He, et al., Dexmedetomidine attenuates neuroinflammation in LPS-stimulated BV2 microglia cells through upregulation of miR-340, *Drug Des. Dev. Ther.* 13 (2019) 3465–3475.
- [22] Liping Wu, Jingtao Chen, Chunsheng Ding, et al., MicroRNA-137 contributes to dampened tumorigenesis in human gastric cancer by targeting AKT2, *PLoS One* 10 (6) (2015) e0130124.
- [23] Kristen Therese Thomas, Bart Russell Anderson, Niraj Shah, et al., Inhibition of the schizophrenia-associated MicroRNA miR-137 disrupts Nrg1alpha neurodevelopmental signal transduction, *Cell Rep.* 20 (1) (2017) 1–12.
- [24] Karelle Leroy, J.-P. Brion, Developmental expression and localization of glycogen synthase kinase-3b in rat brain, *J. Chem. Neuroanat.* 16 (1999) 279–293.
- [25] Xu-Hua Ge, Guo-Ji Zhu, De-Qin Geng, et al., Erythropoietin attenuates 6-hydroxydopamine-induced apoptosis via glycogen synthase kinase 3beta-mediated mitochondrial translocation of Bax in PC12 cells, *Neuro. Sci.* 33 (6) (2012) 1249–1256.
- [26] Jianzhong Zhu, Xue Xu, Yingyin Liang, et al., Downregulation of microRNA-15b-5p targeting the akt3-mediated GSK-3beta/beta-catenin signaling pathway inhibits cell apoptosis in Parkinson's disease, *BioMed Res. Int.* 2021 (2021) 8814862.
- [27] B. Inkster, G. Zai, G. Lewis, et al., GSK3β: a plausible mechanism of cognitive and hippocampal changes induced by erythropoietin treatment in mood disorders? *Transl. Psychiatry* 8 (1) (2018) 216.
- [28] Jinsheng Liu, Li Li, Ping Xie, et al., Sevoflurane induced neurotoxicity in neonatal mice links to a GSK3beta/Drp1-dependent mitochondrial fission and apoptosis, *Free Radic. Biol. Med.* 181 (2022) 72–81.
- [29] N. Wang, Y. Lu, K. Wang, et al., Simvastatin attenuates neurogenetic damage and improves neurocognitive deficits induced by isoflurane in neonatal rats, *Cell. Physiol. Biochem.* 46 (2) (2018) 618–632.
- [30] Robert D. Sanders, J. Xu, Y. Shu, et al., Dexmedetomidine attenuates isoflurane-induced neurocognitive impairment in neonatal rats, *Anesthesiology* 110 (5) (2009) 1077–1085.
- [31] X. Hu, Q. Chi, D. Wang, et al., Hydrogen sulfide inhalation-induced immune damage is involved in oxidative stress, inflammation, apoptosis and the Th1/Th2 imbalance in broiler bursa of Fabricius, *Ecotoxicol. Environ. Saf.* 164 (2018) 201–209.
- [32] M. Li, T.Z. You, W.J. Zhu, et al., Antioxidant response and histopathological changes in brain tissue of pigeon exposed to avermectin, *Ecotoxicology* 22 (8) (2013) 1241–1254.
- [33] Z. Xie, Y. Dong, U. Maeda, et al., The common inhalation anesthetic isoflurane induces apoptosis and increases amyloid β protein levels, *Anesthesiology* 104 (5) (2006) 988–994.
- [34] W. Sun, Y. Lei, Z. Jiang, et al., BPA and low-Se exacerbate apoptosis and mitophagy in chicken pancreatic cells by regulating the PTEN/PI3K/AKT/mTOR pathway, *J. Adv. Res.* (2024).
- [35] B. Li, Y. Zhao, M. Song, et al., Role of c-Myc/chloride intracellular channel 4 pathway in lipopolysaccharide-induced neurodegenerative diseases, *Toxicology* 429 (2020) 152312.
- [36] J. Carmichael, K.L. Sugars, Y.P. Bao, et al., Glycogen synthase kinase-3beta inhibitors prevent cellular polyglutamine toxicity caused by the Huntington's disease mutation, *J. Biol. Chem.* 277 (37) (2002) 33791–33798.
- [37] Linlin Chen, Bin Zhang, Shiqiang Shan, et al., Neuroprotective effects of vitexin against isoflurane-induced neurotoxicity by targeting the TRPV1 and NR2B signaling pathways, *Mol. Med. Rep.* 14 (6) (2016) 5607–5613.
- [38] Hisham F. Bahmad, Batoul Darwish, Karem Bou Dargham, et al., Role of MicroRNAs in anesthesia-induced neurotoxicity in animal models and neuronal cultures: a systematic review, *Neurotox. Res.* 37 (3) (2020) 479–490.
- [39] M. Zhang, D.J. Ge, Z. Su, et al., miR-137 alleviates focal cerebral ischemic injury in rats by regulating JAK1/STAT1 signaling pathway, *Hum. Exp. Toxicol.* 39 (6) (2020) 816–827.
- [40] Shi-yong Li, Xin Chen, Ye-ling Chen, et al., Role of GSK-3beta in isoflurane-induced neuroinflammation and cognitive dysfunction in aged rats, *J. Huazhong Univ. Sci. Technol.* 33 (4) (2013) 530–535.
- [41] G. Tao, Q. Xue, Y. Luo, et al., Isoflurane is more deleterious to developing brain than desflurane: the role of the akt/GSK3β signaling pathway, *BioMed Res. Int.* 2016 (2016) 7919640.
- [42] Marco Sifringer, Clarissa von Haefen, Maria Krain, et al., Neuroprotective effect of dexmedetomidine on hyperoxia-induced toxicity in the neonatal rat brain, *Oxid. Med. Cell. Longev.* 2015 (2015) 530371.
- [43] F. Bao, X. Kang, Q. Xie, et al., HIF-α/PKM2 and PI3K-AKT pathways involved in the protection by dexmedetomidine against isoflurane or bupivacaine-induced apoptosis in hippocampal neuronal HT22 cells, *Exp. Ther. Med.* 17 (1) (2019) 63–70.
- [44] Y. Zhu, P. Zhao, L. Sun, et al., Overexpression of circRNA SNRK targets miR-103-3p to reduce apoptosis and promote cardiac repair through GSK3β/β-catenin pathway in rats with myocardial infarction, *Cell Death Dis.* 7 (1) (2021) 84.
- [45] Susan A. Farra, Jessica L. Ripley, Rukhsana Sultan, et al., Antisense oligonucleotide against GSK-3beta in brain of SAMP8 mice improves learning and memory and decreases oxidative stress: involvement of transcription factor Nrf2 and implications for Alzheimer disease, *Free Radic. Biol. Med.* 67 (2014) 387–395.
- [46] Eléonore Beurel, R.S. Jope, The paradoxical pro- and anti-apoptotic actions of GSK3 in the intrinsic and extrinsic apoptosis signaling pathways, *Prog. Neurobiol.* 79 (4) (2006) 173–189.
- [47] S. Fukumoto, C.-M. Hsieh, K. Maemura, et al., Akt participation in the Wnt signaling pathway through Dishevelled, *J. Biol. Chem.* 276 (20) (2001) 17479–17483.
- [48] S.P. Monga, H.K. Monga, X. Tan, et al., Beta-catenin antisense studies in embryonic liver cultures: role in proliferation, apoptosis, and lineage specification, *Gastroenterology* 124 (1) (2003) 202–216.
- [49] Y.Z. Chen, APP induces neuronal apoptosis through APP-BP1-mediated downregulation of beta-catenin, *Apoptosis* 9 (4) (2004) 415–422.

- [50] L. Yang, K. Kang, Y. Lin, et al., Up-regulation of miR-137 can inhibit PTN in target manner to regulate PTN/PTPRZ pathway to prevent cognitive dysfunction caused by propofol, *Am J Transl Res* 12 (11) (2020) 7490–7500.
- [51] Q.Q. Wu, B. Zheng, G.B. Weng, et al., Downregulated NOX4 underlies a novel inhibitory role of microRNA-137 in prostate cancer, *J. Cell. Biochem.* 120 (6) (2019) 10215–10227.
- [52] W. Li, X. Bai, R. Guo, et al., MicroRNA-137 inhibits esophageal squamous cell carcinoma by down-regulating DAAM1, *Protein Pept. Lett.* (2022).